Summer Internship Programme (2018) on-

SILICON PHOTONICS AND WAVEGUIDE BRAGG GRATINGS

By-

Sai Vaibhav Naidu

Ramaiah Institute of Technology,

Bangalore-560012.

Under the guidence of-

Dr. Srinivas Talabattula

Electronics and communications Department,

Indian Institute of Science,

Banglore-560012.

Overview:

Abstract

1. Waveguides

1.1 Design

1.2 Theory

2. Silicon Photonics

2.1 Introduction 2.2 Light emission

2.3 Quantum confinement of electrons 2.4 Ramen scattering

2.5 Erbium Doping 2.6 Photodetectors

2.7 Advantages

3. Advancements in Silicon Photonics

3.1 Introduction 3.2 Silicon Photonics Passives

3.3 Heterogeneous silicon Photonics 3.4 Single-wavelength lasers

4. Gratings

4.1 Introduction 4.2 Design and Fabrication

4.3 Bragg gratings on ridge waveguide 4.4 Design layout

Simulation

Conclusion

References

Acknowledgement

Abstract

The Silicon Photonics has its origins in the late 1980s and early 1990s, only in the last three years has the field developed significant momentum, so much so that we can expect an explosion of applications and technical developments in the next decade. Most promising are applications in the fields of optical interconnects, low-cost telecommunications, and optical sensors, perhaps including disposable biosensors. As the field of silicon photonics becomes more mature, foundry processes will be an essential piece of the ecosystem for eliminating process risk and allowing the community to focus on adding value through clever design.

1. Waveguides

1.1 Design

The basic structure of a 2-D (or slab) waveguide is shown below with the index profiles along the depth, where the indices of the cladding layer, guiding layer, and substrate are nc, nf, and ns, respectively. In the case that $n_f > n_s > n_c$, the light is confined in the guiding layer by the total internal reflections at two interfaces and propagates along a zigzag path. Such a confined lightwave is called a guided mode whose propagation constant β along the z direction exists in the range of $k_0 n_s < \beta < k_0 n_f$, where $k_0 = 2\pi/\lambda$.

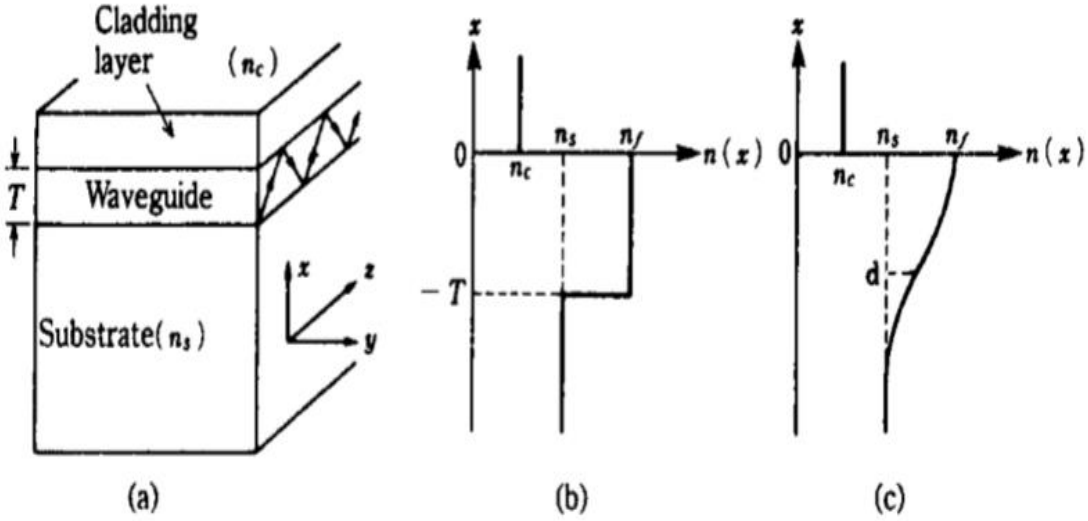

Fig 1.1 2-D optical waveguides. (a) The basic optical-waveguide structure; (b) the step-index type; and (c) the graded-index type.

1.2 Theory

The asymmetric measure of the waveguide is also defined as,

$$a_E = \frac{(n_s^2 - n_c^2)}{(n_f^2 - n_s^2)}$$

when $n_s = n_c$, $a_E = 0$. This implies symmetric waveguides.

Wave equation can be derived from Maxwell's equation,

$$\nabla^2\Psi = \frac{1}{v^2}\frac{\partial^2\Psi}{\partial t^2}$$

Where Ψ is mode field.

So we get a equation in which there are two variables

$$\frac{\partial^2\Psi}{\partial x^2} + \frac{\partial^2\Psi}{\partial y^2} + (k_0^2 n^2 - \beta^2)\Psi = 0$$

Where k_0 is $2\pi/\lambda$, and n is refractive index.

For 2-D waveguide neglect y-axis,

$$\frac{\partial^2\Psi}{\partial x^2} + (k_0^2 n^2 - \beta^2)\Psi = 0$$

Scalar wave approach- where slab waveguides are studied in which only one component is given priority and other components can be derieved by it.

So the above equation can be written separately for core and cladding region and then match them.

$$\frac{\partial^2\Psi_1}{\partial x^2} + (k_0^2 n_1^2 - \beta^2)\Psi_1 = 0 \qquad \text{,for core region}$$

$$\frac{\partial^2\Psi_2}{\partial x^2} + (k_0^2 n_2^2 - \beta^2)\Psi_2 = 0 \qquad \text{,for cladding region}$$

We can take $k^2 = (k_0^2 n_1^2 - \beta^2) | \alpha^2 = -(k_0^2 n_2^2 - \beta^2)$

By applying boundary condition we get,

$$\Psi(x) = \begin{cases} B\cos kx & , |x| < w/2 \\ De^{-\alpha x} & , |x| > w/2 \end{cases}$$

$$\text{and,} \qquad \Psi'(x) = \begin{cases} -k\,B\sin kx & , |x| < w/2 \\ -\alpha\,De^{-\alpha x} & , |x| > w/2 \end{cases}$$

Finally we get,

$$k \tan k \frac{w}{2} = \alpha$$

This is a transcendental equation to obtain β.

The v-parameter of the waveguide is given by,

$$v = k_0 \frac{w}{2} \sqrt{n_1^2 - n_2^2}$$

v determines the mode of the waveguide.

And by this we can have a v-b curve

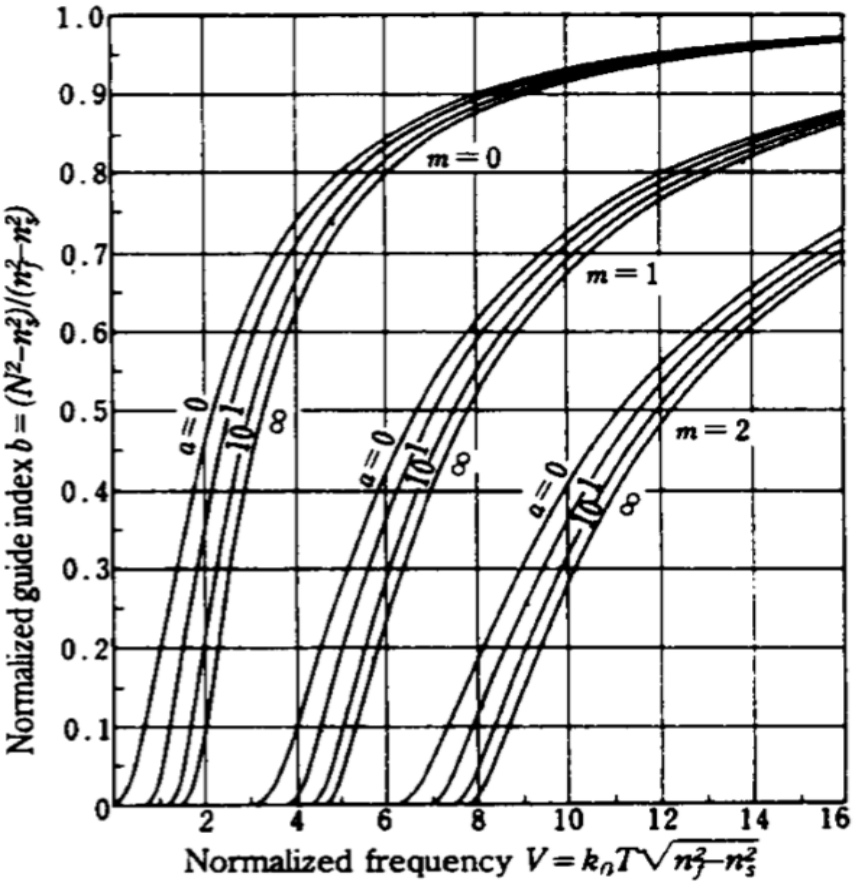

Fig1.2 Dispersion curve for step index 2-D waveguide

We can find out, for a given waveguide specifications (like refractive index and width) how many modes is supported by it as shown in Fig1.2

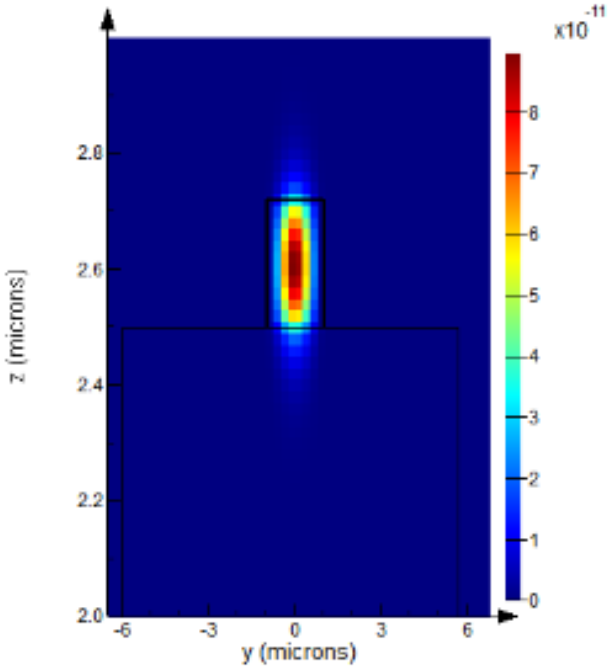

Fig1.3 Simulation of asymmetric waveguide

This shows that the waveguide is single mode with effective index 2.80 and the light is confined inside the core region and no loss occurs.

2. Silicon Photonics

2.1 Introduction

Silicon photonics is an evolving technology in which data is transferred among computer chips by optical rays. Optical rays can carry far more data in less time than electrical conductors. Most promising applications are optical interconnects, low cost telecommunications, optical sensors, modulators, etc.

Driven by the large dynamic range in microwave photonic systems, components must exhibit low noise, high linearity and high saturation power which are achieved using silicon. After silicon etches, ion implantation and germanium growth, the metal stack is fabricated. The back-end includes patterning of the metal vias, contacts, interconnects and pads.

2.2 Light emission

The creation of silicon light emitters and lasers has potential payoff as well as the significant challenge posed by nature. The challenge has to do with bulk crystalline silicon being an indirect bandgap material, which means that the upper and the lower electronic states (conduction and valence bands) do not have the same value of momentum. Because the photon of interest has

negligible momentum compared to that of the electron, the electron-hole recombination needs to be mediated by emitting or absorbing a phonon to conserve momentum. In the terminology of quantum mechanics, this is a second-order process, which implies that, although not forbidden, the probability of occurrence is extremely low.

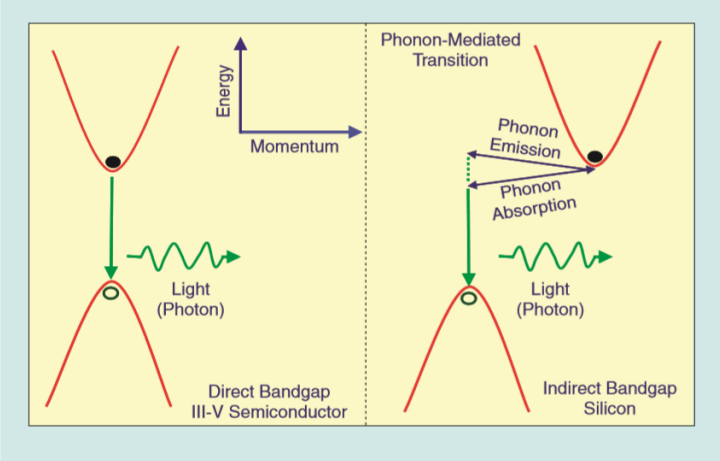

Fig2.1 In a direct bandgap material, e.g. GaAs, electrons in the conduction band recombine with the holes in the valence band, transferring their energies to emitted photons. In an indirect bandgap material, e.g., silicon, the recombination is mediated by absorption or emission of a phonon

Approaches aimed at overcoming or circumventing this limitation, most belong to one of three main categories:

- overcoming the indirect band structure by using spatial confinement of the electron.
- introduction of rare earth impurities as optically active dopants.
- the use of Raman scattering to achieve optical gain.

2.3 Quantum confinement of electrons

When a conduction electron is free to roam the silicon crystal, its momentum is well defined. Spatial confinement of the electron within a silicon nanocrystal (NC) creates an ambiguity in the value of its momentum, a phenomenon that is referred to as the Heisenberg uncertainty principle. When the amount of this momentum ambiguity approaches the initial momentum mismatch, momentum conservation is relaxed, and the efficiency of light emission increases. A thin film of silica (SiO_2) impregnated silicon NCs is the most common approach for confinement of electrons.The emission wavelength is below the band edge of silicon, implying that the light produced cannot propagate in a silicon waveguide since bulk silicon is opaque at these wavelengths. Another limitation is that the propagation losses will be high due to light scattering from the NCs, which have a much higher refractive index (3.5) compared to the SiO_2 host.

2.4 Raman Scattering

The use of Raman scattering to overcome the indirect band structure of silicon was proposed in 2002 as an alternative to the approaches. The advantage of this technique is the ability to use pure silicon without the need for NCs or Er doping; therefore, it is fully compatible with silicon microelectronics manufacturing. The traditional limitation of the Raman approach is that it cannot be electrically excited and requires an off-chip pump.

2.5 Erbium Doping

Erbium (Er)-doped fiber amplifiers and lasers have become successful commercial technologies to the extent that such amplifiers are standard building blocks of fiber-optic networks. Rendering silicon optically active by doping it with Er proved to be unsuccessful due to the limited solid solubility and the competition from non-radiative processes, including back transfer of energy from Er to silicon.

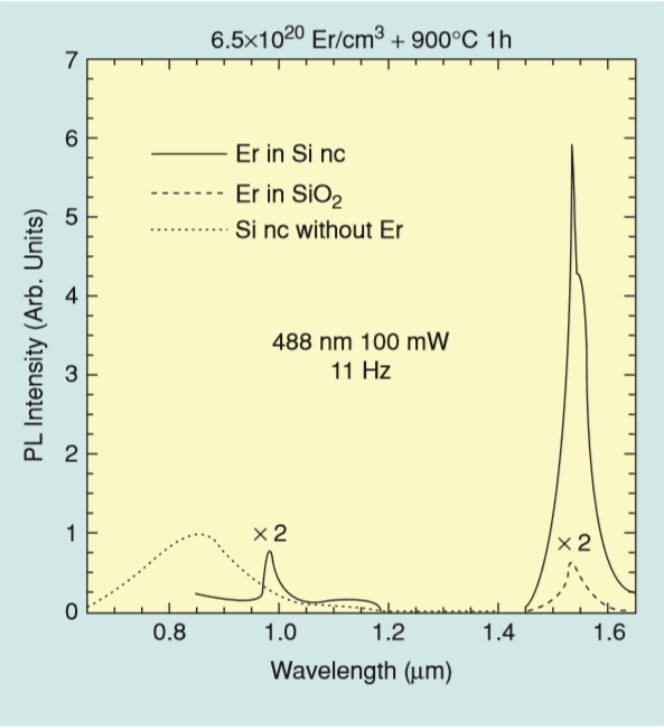

Fig2.2 Emission spectrum of silicon NCs embedded in a silica film (dotted); of Er in a silica film (dashed); and of Er in presence of NCs, both embedded in a silica film (solid)

A typical luminescence spectrum is shown in Figure 2.2 (dashed line), exhibiting emission centred in the 1.55-μm wavelength band (C-band). Corresponding to the low attenuation window of optical fibres, this is one of the most important wavelength bands for optical communication.

An apparent disadvantage of silica as a host for Er is that, being an insulator, it cannot be electrically pumped using an integrated diode.

2.6 Photodectors

Silicon-based PDs are commonly used for applications that operate in the visible spectrum due to their near-perfect efficiency at these visible wavelengths. Most communication wavelengths are centered in the near-infrared wavelengths of 1.31 and 1.55 µm, a region where silicon is a poor detector. To improve the performance of silicon-based detectors, the most common approach is to introduce germanium (Ge) to the material system to reduce the bandgap.

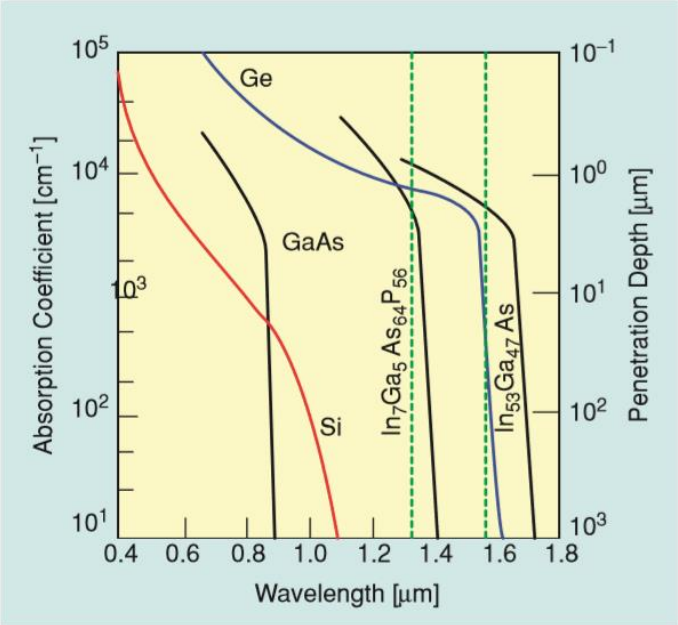

Fig2.3 Absorption coefficient and penetration depth of various bulk materials as a function of wavelength. The green lines mark typical wavelengths for telecommunications windows of 1.310 and 1.550 µm.

The effect on the absorption coefficient and penetration depth, defined as the distance that light travels before the intensity falls to 36% (1/e), is shown in Figure2.3.

2.7 Advantages

High data transfer because of increased bandwidth.

Photonics + Electronics together can enable solutions that can achieve higher degree of data transfer [1 Tb/s] with low cost.

They have high refractive index and 1/500th times as thin as conventional waveguides

3. Advancements in Silicon Photonics

3.1 Introduction

The objective here is to highlight recent progress and trends in the development of silicon photonics. The trend is to use optics in intimate proximity to the electronic circuit, which implies a high level of optoelectronic integration.

This evolution toward silicon based technologies is largely based on the vision that silicon provides a mature integration platform supported by the enormous existing CMOS manufacturing infrastructure, which can be used to cost-effectively produce integrated optoelectronic circuits for a wide range of applications, including telecommunications, optical interconnects, medical screening, spectroscopy, and biological and chemical sensing.

3.2 Silicon Photonics Passives

Silicon and its oxide form high-index contrast, high-confinement waveguides ideally suited for medium to high-integration and small passive devices in their transparency wavelength range. The measured loss is still limited by bend loss in this low-confinement configuration with very low sidewall interaction, so the pure propagation loss could be even lower.

Using two waveguide types (silicon nitride and silicon), the prohibitively high material losses that would be present in a single waveguide platform for UV to midIR wavelengths are avoided while providing a platform compatible with heterogeneous integration of laser sources covering the same spectral range.

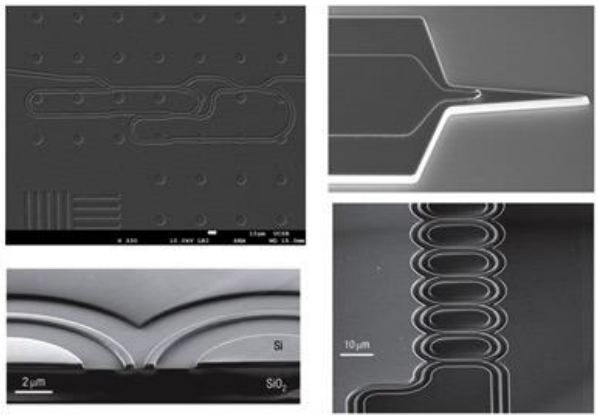

Fig3.1 Si/SiO2 material system offers superior waveguide capabilities due to high index contrast and maturity of Si processing allowing for very small wires and tight bends

Record low losses in silicon, less than 3 dB/m at 1600 nm, have been reported in, calculated by the internal Q factor of silicon ring resonators of 2.2x107. Such record values are probably not suitable for wide integration as the radius of said ring was 2.45 mm. By increasing the confinement, the bend loss goes down at the expense of higher propagation loss, mainly due to scattering at vertical

sidewalls. Nevertheless, complex devices with much smaller bend radii and measured propagation loss <0.5 dB/cm in C-band and <0.7 dB/cm in O-band have been demonstrated.

3.3 Heterogeneous Silicon Photonics

Heterogeneous silicon photonics, due to its potential for medium- and large-scale integration, has been intensively researched. Recent developments have shown that heterogeneous integration not only allows for a reduced cost due to economy of scale, but also allows for same or even better performing devices than what has previously been demonstrated utilizing only III-V materials.

It has potential for bringing the large wafer size, volume throughput, and cost reduction of silicon manufacturing to photonic components.

The silicon-on-insulator (SOI) platform fabrication infrastructure is compatible with CMOS technology and is highly accurate and mature, leading to a robust, high yield and reproducible technology.

Because of indirect bandgap of silicon, electrically pumped efficient sources for silicon is a challenge.

We can use III-V gain regions which are directly placed on silicon surface to effeciently introduce electrically pumped sources.

First approach is using III-V chips bonded on silicon with coarse alignment and subsequently processed on the Si wafer scale. This has the advantage of minimizing the area requirement of III-V material, thus minimizing the III-V epitaxial wafer cost. It has also the great advantage that very different epitaxial stacks can be integrated together and processed simultaneously.

Second approach is the direct epitaxial growth of III-V layers on silicon or SOI using intermediate buffer layers to minimize dislocations propagating into the active region.

The use of quantum dot (QD) laser gain material can minimize the effect of threading dislocations on threshold and output power, as efficient capture and localization of injected carriers by individual quantum dots greatly reduces non-radiative recombination at dislocations.Heterogeneous integration on silicon can also accommodate exotic materials such as LiNbO3 bringing the promise of high performance modulators, nonlinearities and magnetic properties.

Light generation on silicon chips can also be achieved by integration of rare-earth-ion (RE) doped dielectric thin films.

The advantages of RE approach would be-

-direct deposition onto silicon substrates

-amplification of higher bit-rate signals without patterning effects

-higher temperature of operation and inherent narrow linewidth.

Disadvantages are, significantly lower gain in range of few dB/cm and a need for optical pumping.

3.4 Single-wavelength lasers

The linewidth of single-frequency semiconductor lasers is inherently broader than of solid-state lasers.

In a semiconductor laser there are two mechanisms broadening the linewidth-

(1) The spontaneous emission which alters the phase and intensity of lasing field

(2) The linewidth enhancement factor α that characterizes the coupling between intensity and phase noise and is specific to semiconductor lasers due to carrier density fluctuations.

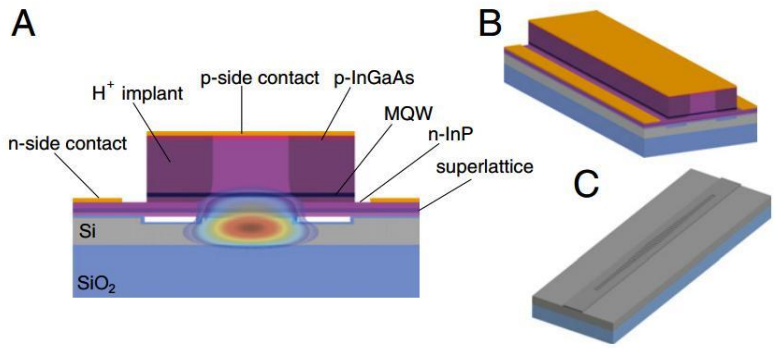

Fig3.2 (A) Two-dimensional cross-section of the heterogeneous platform, with superimposed optical transverse mode profile.(B) Perspective view of a high-Q heterogeneous laser.(C) Perspective view of the high-Q silicon resonator

The total Q of a heterogeneous resonator can then be expressed as:

$$\frac{1}{Q} = \frac{\Gamma}{Q_{III-V}} + \frac{1-\Gamma}{Qsi}$$

Where Γ is the mode confinement factor in III-V. By tailoring the transverse geometry, the modal confinement can be engineered and total Q can be optimized for best performance. Increasing the quality factor of the laser cavity and keeping the same modal confinement provides a double benefit to phase noise by reducing the number of excited carriers needed to reach threshold, thus decreasing spontaneous photon generation while increasing photon storage. By designing a high-Q silicon resonator with Q = 1.1×10^6 and having a Γ = 15%, linewidths as low as 18 kHz can be created.

4. Gratings

4.1 Introduction

Periodic structures or gratings in waveguide are one of the most important elements for OICs, since they can perform various passive functions and provide effective means of guided-wave control. Typically, the grating is achieved by physically corrugating the silicon waveguide. The two waveguide structures that are most commonly used for integrated gratings: strip and ridge waveguides with corrugations on them.

Strip waveguides, or photonic wires, usually have submicron cross sections (e.g., 220 nm thick and 500 nm wide) and light is strongly confined in the core, due to the high refractive index contrast between the core (silicon) and the cladding (oxide or air). The grating corrugations are normally on the waveguide sidewalls, so the grating and waveguide can be defined in a single lithography step. Due to the small waveguide dimensions and optical mode size, a small perturbation on the sidewalls can cause a considerable grating coupling coefficient. Therefore, it is difficult to obtain a narrow reflection/filtering bandwidth. The lowest bandwidth for strip waveguide Bragg gratings is ~0.8 nm with a corrugation width of 10 nm.

Ridge waveguides, on the other hand, typically have much larger cross sections (e.g., a few microns), thus allowing higher fabrication tolerance. The gratings can be achieved by corrugating the top surface or the sidewalls, where the sidewalls can be corrugated either on the ridge or on the slab. In contrast to the top surface gratings with a fixed etch depth, the sidewall-corrugated configuration has the advantage that the corrugation width can be easily controlled. Main aim is to achieve a Narrow-Bandwidth Bragg agratings on SOI wafers with CMOS-compatible fabrication.

4.2 Design and Fabrication

The silicon ridge waveguide is on top of a 2 μm buried oxide layer. The total height (H) and width (w_2) of the waveguide are 220 nm and 1 μm, respectively. The shallow-etched ridge width (w_1) is 500 nm and the etch depth (D) is 70 nm. The devices were fabricated at IMEC using a CMOS compatible process with 193 nm deep ultraviolet (UV) lithography.

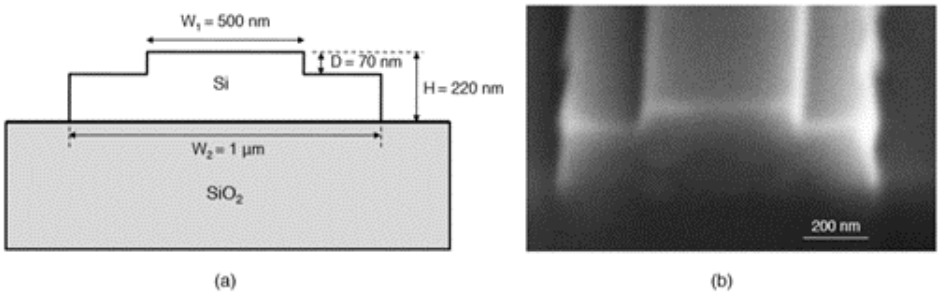

Fig4.1 (a) Schematic diagram of the cross section of the ridge waveguide. (b) Tilted SEM image of a fabricated device with corrugations on the slab.

It can be seen that the cross section profile is not perfectly rectangular and has slightly sloped sidewalls. Such geometric imperfections will affect the effective index of the waveguide, and, consequently, shift the Bragg wavelength from its design value.

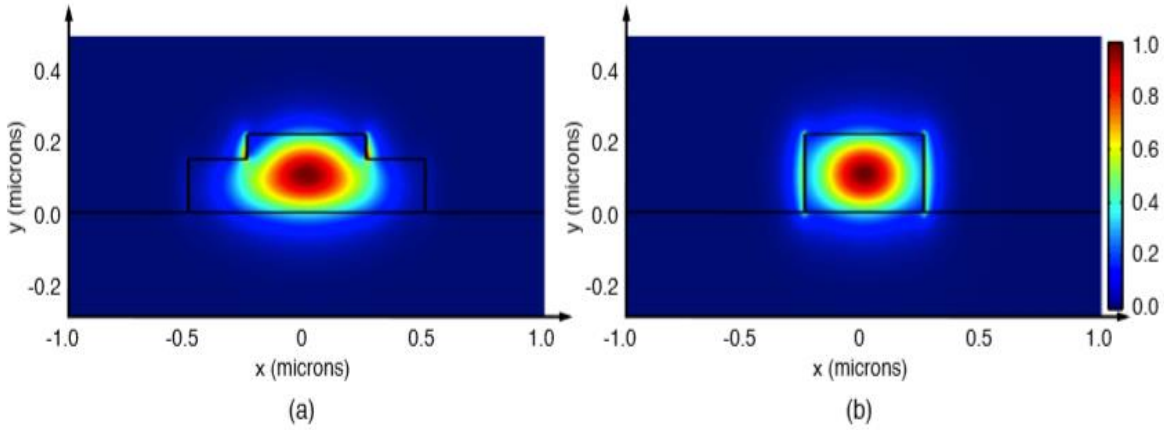

Fig4.2 Simulated fundamental TE mode profile. (a) Ridge waveguide. (b) Strip waveguide.

4.3 Bragg gratings on ridge waveguide

The gratings are realized by introducing periodic sidewall corrugations either on the ridge or on the slab. The grating period Λ was designed to be 290 nm, with a duty cycle of 50%, resulting in an expected Bragg wavelength around 1526 nm. The total length of the gratings L is 580 μ m, i.e., 2000 grating periods. Symmetric corrugations (relative to the non-grating waveguide edges) can be used so that the average effective index is approximately constant.

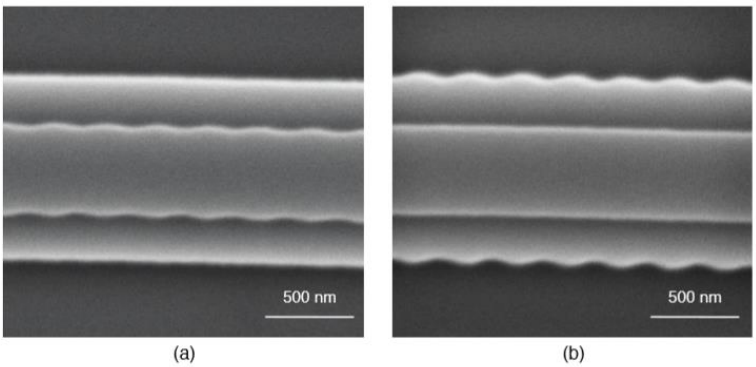

Fig4.3. Top view SEM images of Bragg gratings fabricated on ridge waveguides. (a) Grating on the ridge: corrugation width on each side is 60 nm. (b) Grating on the slab: corrugation width on each side is 80 nm.

4.4 Device Layout

The device layout schematic for input and output ports, integrated waveguide-to-fiber grating couplers can be used which were designed for TE polarization.

To collect the reflected light, a Y-branch splitter was placed between the input grating coupler and our gratings. A 500 nm strip waveguide can be used for the routing waveguides as well as for the Y-branch splitter in order to minimize their footprints and bending losses. Since the gratings are on the ridge waveguide, a double-layer linear taper is designed for the transition between the strip and ridge waveguides. As shown in the figure, the taper section connects the strip waveguide and the ridge waveguide gratings and is 30 μ m long to ensure that the transition loss is negligible.

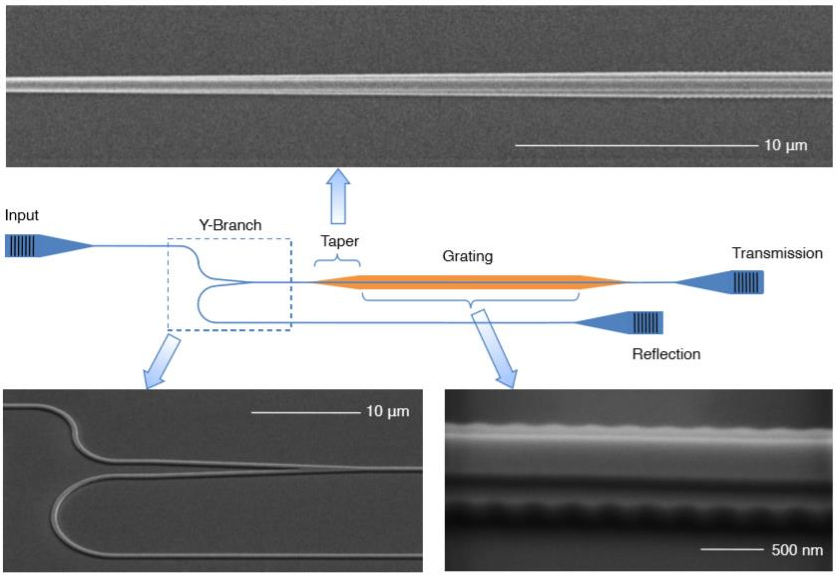

Fig4.4 Schematic diagram of the device layout and SEM images of each of the components

4.5 Measurements

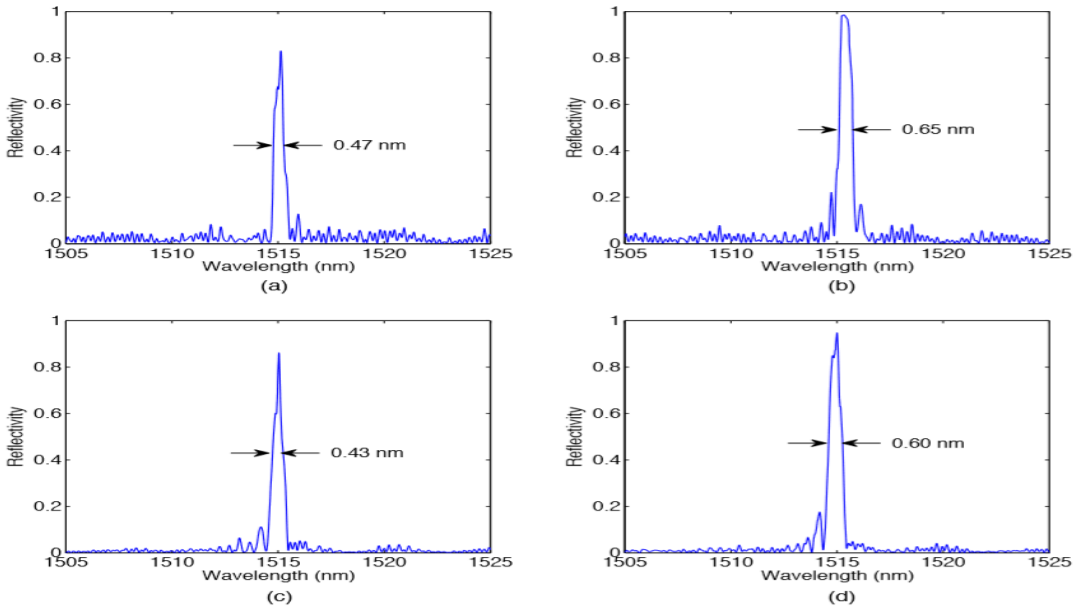

Fig4.5 Measured reflection spectra of the Bragg gratings fabricated on ridge waveguides. (a) Grating on ridge with 40 nm corrugations. (b) Grating on ridge with 60 nm corrugations. (c) Grating on slab with 40 nm corrugations. (d) Grating on slab with 60 nm corrugations.

It can be observed that the two configurations show similar performance, although the 3-dB bandwidths are slightly smaller for gratings on the slab than for gratings on the ridge, which can be attributed to the fact that the optical field distribution at the slab sidewalls is slightly less than at the ridge sidewalls. The measured Bragg wavelength is roughly constant at about 1515 nm, which is shorter than the design value (~1526 nm). This blue shift in the Bragg wavelength is due to the fact that the fabricated waveguide is more like a slightly smaller trapezoid instead of the perfect rectangular shape, which results in a lower effective index. By using 60 nm corrugations, a peak reflectivity of greater than 90% was achieved in both configurations. As the corrugation width is reduced to 40 nm, the bandwidth becomes smaller and the reflectivity decreases. To increase the reflectivity, longer gratings should be used.

We can find the peak reflectivity and bandwidth mathematically,

$$R = \tan h^2(\kappa L)$$

$$\Delta\lambda = \frac{\lambda_0^2}{\pi n_g}\sqrt{k^2 + (\pi / L)^2}$$

Where R is the peak reflectivity, κ is the coupling coefficient, Δ λ is the bandwidth at the first nulls, λ 0 is the Bragg wavelength, and ng is the group index.

The waveguide geometry is usually designed to be single-mode. Single-mode ridge waveguide can have higher order leaky modes, which lead to unwanted dips in the transmission spectrum on the shorter wavelength side of the fundamental mode. To increase the spectral separation of these leaky modes from the fundamental mode, it is necessary to shrink the waveguide dimensions.

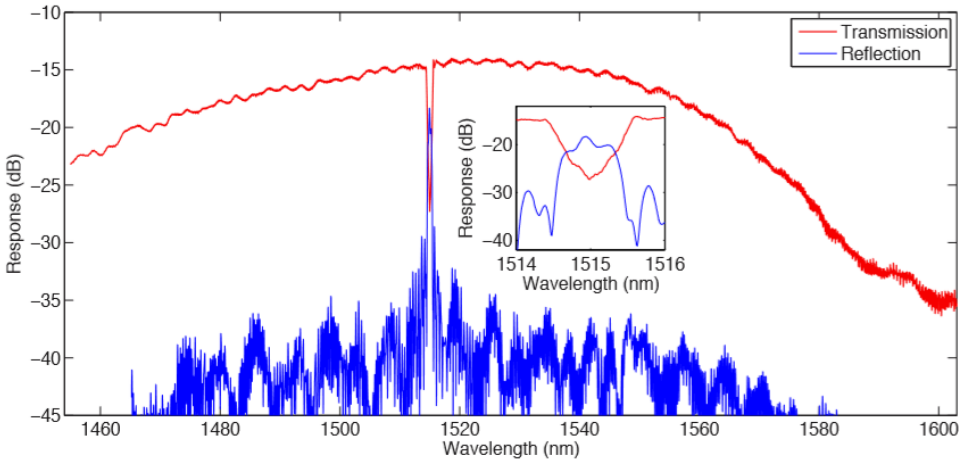

Fig4.6 Measured spectral responses of the Bragg grating on ridge waveguides designed with 80 nm corrugations on the slab. The spectra are plotted without normalization. The inset shows the enlarged plot around the Bragg wavelength.

The measured bandwidth is plotted as a function of the designed corrugation width in Fig4.7 for each of the three grating structures on the same die. We can see that the green curve (strip waveguide gratings) has a much higher slope than the other two curves (ridge waveguide gratings).

To obtain a bandwidth below 1 nm, if using the strip waveguide, then a corrugation width less than 10 nm will be required, whereas, if using the slab region of the ridge waveguide, then an 80 nm corrugation width should be enough. For the ridge waveguide gratings, the slope is almost the same for the two configurations, and the 3-dB bandwidth ranges from 0.4 nm to 0.75 nm, which makes the devices suitable for many narrow-band applications.

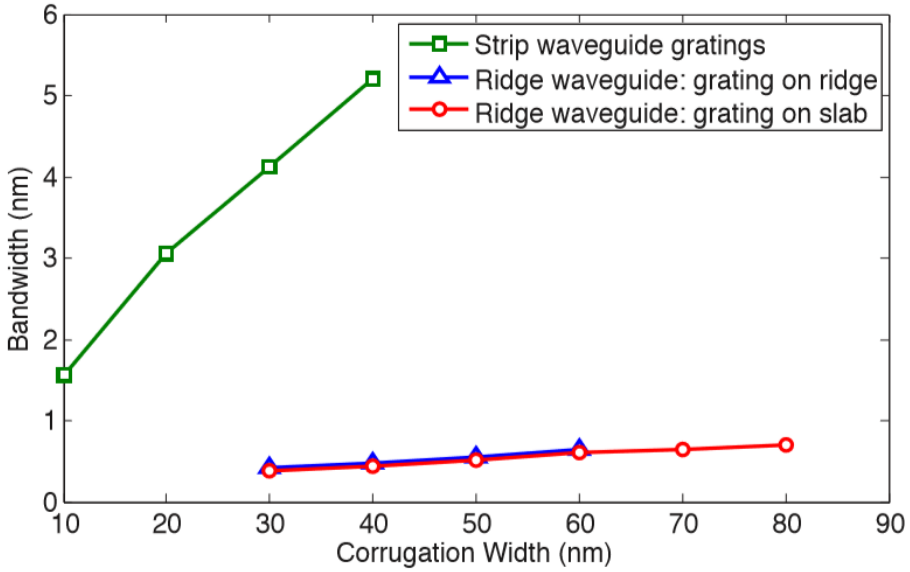

Fig4.7 Measured 3-dB bandwidth versus the designed corrugation width for different grating structures on the same die.

Simulations

Ring resonators using Interconnect

Here I am implementing a single Ring resonator using 2 couplers and 2 strip waveguides connected as shown below.

The input source is given port 2 of c1 and the out is observed at port 1 of c2 as the light enters the component and goes around a number of times and comes out of port 1 of c2.

In case of a double ring resonator, the output will be observed at port 3 of c2 due to the presence of one more ring in the structure.

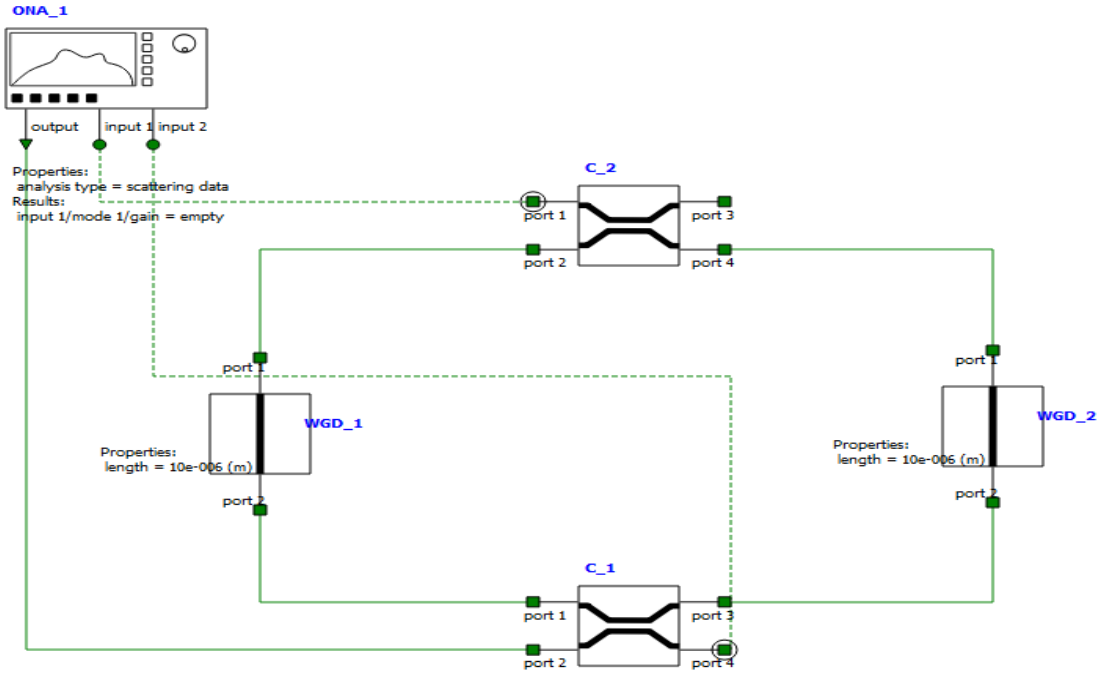

Here the frequency range is set to 100 THz with center frequency of 1 THz

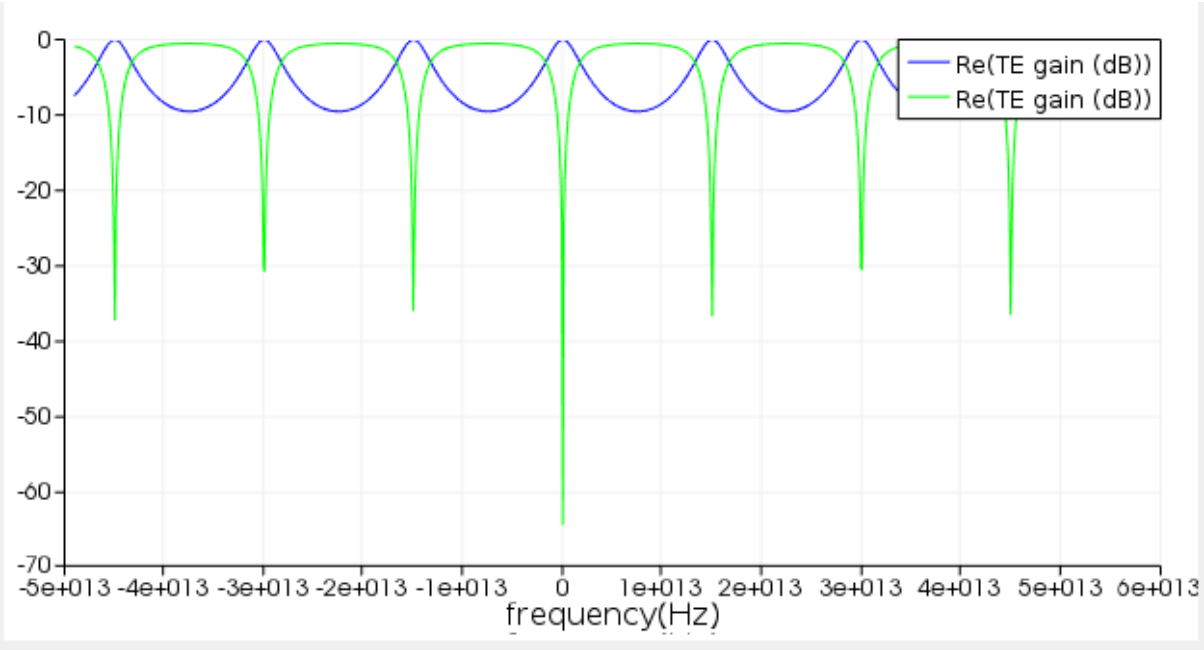

The resonant frequency of the wavelength which propagates inside the ring and comes out of port 1 of c2 in the above simulation is shown in blue line and the wavelength which are not resonant with the ring resonator and comes out of port 4 of c1 is shown by green line.

Grating coupler

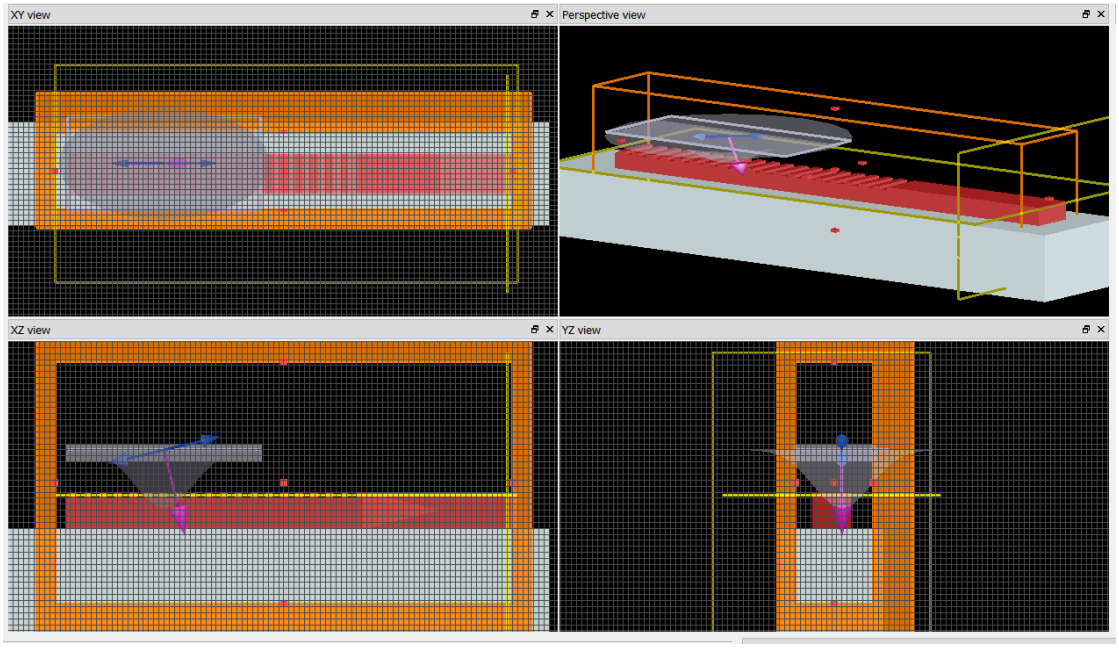

The model is done by using FDTD solutions of Lumerical software. A silicon oxide is used as substrate on top of which there is a silicon waveguide with a grating coupler.

A Gaussian source of centre wavelength 1.55 µm and wavelength span of 0.05 µm at an angle -13.5 is used. We will be analysing the energy propagation at the end of the waveguide by keeping a monitor at its end.

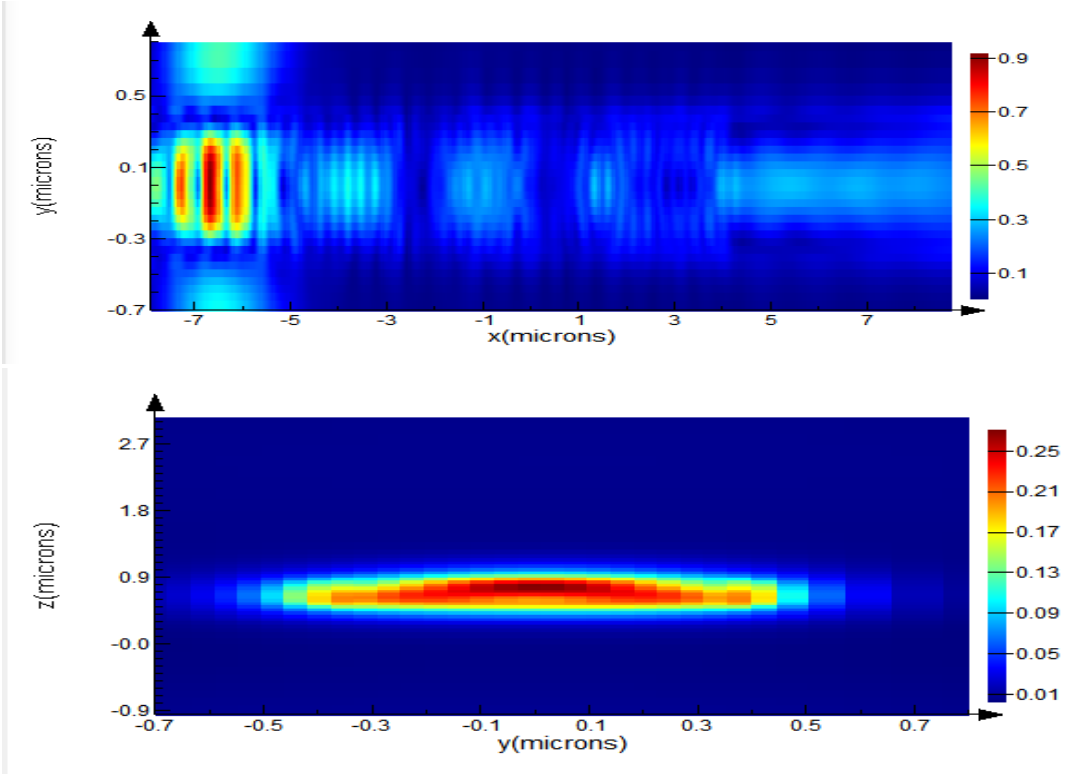

The light is propagating along z-axis and getting coupled into the waveguide. We can observe some losses due to improper dimensions in taper. I will further simulate to give 100% result.

Asymmetric Waveguide

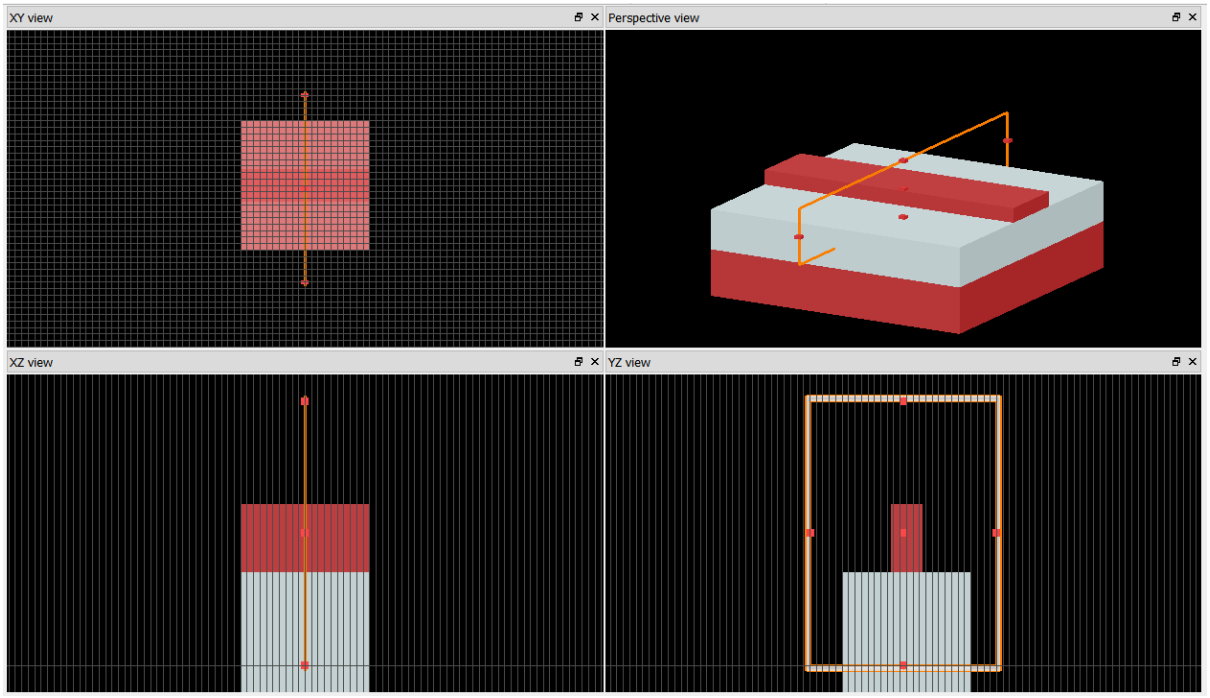

This is a simulation in mode solutions of asymmetric waveguide where the mode, effective index for a particular mode and thickness of the waveguide are determined.

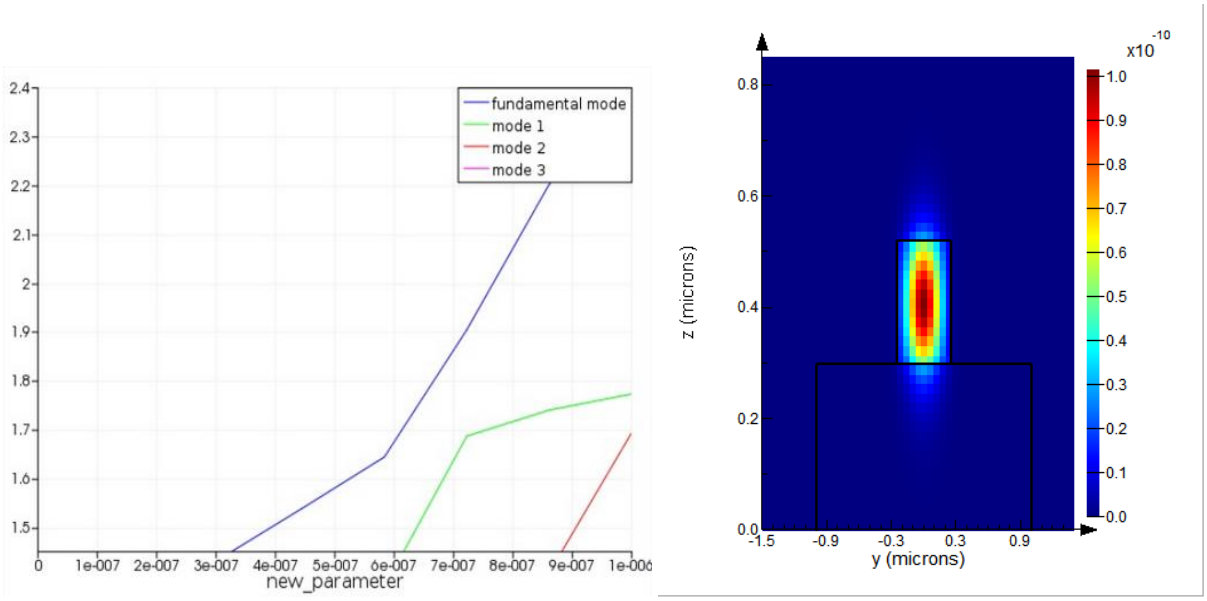

We can see that the light is confined inside the waveguide with no loss.

Conclusion

I would like to conclude by saying that in Linear integrated photonics, Silicon plays a very important role due its low cost and low loss and high bandwidth. Silicon photonics could provide low-cost opto-electronic solutions for applications ranging from telecommunications down to chip-to-chip interconnects.

The gratings are preferred for coupling of light in the waveguide as it is very convenient to fabricate and occupies less space and can propagate narrow bandwidth less than 1 nm unlike other couplers(like butt coupler) which requires a very long slope to couple light, taking up a lot of space on the chip.

Acknowledgement

I would like to thank Indian Institute of Science for granting me the Summer Internship. I am extremely thankful to Dr. Srinivas Talabattula, ECE, IISc, for guiding me throughout this internship. I would like to thank Mr. Yadunath for taking us to the fabrication lab (CENSE) and explaining how things work inside. I also would like to thank Mr. Aniket Patra for helping me learn Lumerical software. I thank all the mentors (Radhika Priyadarshini ma'am, Archana Sharma ma'am, Shafeek sir) for keeping me updated on what's going on around the institute and also for helping me in various other topics.

Reference

1. N. Kobayashi et al., "Silicon Photonic Heterogeneous Ring-Filter External Cavity Wavelength Tunable Lasers," IEEE Journ. of Lightw. Tech., vol. 33, no. 6, pp. 1241-1246, Mar. 2015
2. John E. Bowers*, Sudharsanan Srinivasan, "Recent Advances in Silicon Photonic Integrated Circuits".
3. By Pascual Muñoz, Photonic integrated circuits using generic technologies.
4. K. Takeda, T. Sato, T. Fujii, E. Kuramochi, M. Notomi, K. Hasebe, T. Kakitsuka, and S. Matsuo, "Heterogeneously integrated photonic-crystal lasers on silicon for on/off chip optical interconnects," Opt. Express 23, 702-708 (2015) Proc.
5. Ari Novack*, Matt Streshinsky, "Progress in silicon platforms for integrated optics", 2016.
6. M. Paniccia, "Silicon photonics: Opportunity and integration challenges,"in Proc. 1st Int. Conf. Group IV Photonics, Hong Kong, Sept.2004.
7. P. Herve, and S. Ovadia, "Optical technologies for enterprise networks," Intell. Technol. J., vol. 8, pp. 73–82, 2004.
8. Xu Wang, Department of Electrical and Computer Engineering, University of British Columbia Vancouver, Canada, "Narrow-band waveguide Bragg gratings on SOI wafers with CMOS-compatible fabrication process".